

## Toward Rational Control of Metal Stoichiometry in Heterobimetallic Coordination Complexes: Synthesis and Characterization of $\text{Pb}(\text{Hsal})_2(\text{Cu}(\text{salen}^*))_2$ , $[\text{Pb}(\text{NO}_3)(\text{Cu}(\text{salen}^*))_2](\text{NO}_3)$ , $\text{Pb}(\text{OAc})_2(\text{Cu}(\text{salen}^*))$ , and $[\text{Pb}(\text{OAc})(\text{Ni}(\text{salen}^*))_2](\text{OAc})$

John H. Thurston, Christopher G.-Z. Tang, Daniel W. Trahan, and Kenton H. Whitmire\*

Department of Chemistry, Rice University, 6100 Main Street, Houston, Texas 77005

Received December 12, 2003

The ability of the transition metal complex  $\text{M}(\text{salen}^*)$  ( $\text{M} = \text{Ni}, \text{Cu}$ ) to form Lewis acid–base adducts with lead(II) salts has been explored. The new complexes  $\text{Pb}(\text{Hsal})_2(\text{Cu}(\text{salen}^*))_2$  (**1**),  $\{\text{Pb}(\text{NO}_3)(\text{Cu}(\text{salen}^*))\}_2(\text{NO}_3)$  (**2**),  $\text{Pb}(\text{OAc})_2(\text{Cu}(\text{salen}^*))$  (**3**), and  $\{\text{Pb}(\text{OAc})(\text{Ni}(\text{salen}^*))_2\}(\text{OAc})$  (**4**) ( $\text{Hsal} = \text{O}_2\text{CC}_6\text{H}_4\text{-2-OH}$ ,  $\text{salen}^* = \text{bis}(3\text{-methoxy-salicylideneimine})$ ) have been synthesized and characterized spectroscopically and by single-crystal X-ray diffraction. The coordination environment of the lead in the heterobimetallic complex is sensitive both to the initial lead salt and to the transition metal salen complex that is employed in the synthesis. As a result, we have been able to access both 2:1 and 1:1 adducts by varying either the lead salt or the transition metal in the heterobimetallic coordination complex. In all cases, the  $\text{salen}^*$  complex is associated with the lead center via dative interactions of the phenolic oxygen atoms. The relationship between the coordination requirements of the lead and the chemical nature of the anion is examined. In compound **1**, the  $\text{Pb}^{2+}$  ion is chelated by two  $\text{Cu}(\text{salen}^*)$  moieties, and both salicylate ligands remain attached to the lead center and bridge to the  $\text{Cu}^{2+}$  ions. The two  $\text{Cu}(\text{salen}^*)$  groups are roughly parallel and opposed to each other as required by crystallographic inversion symmetry at lead. In contrast, the two  $\text{Cu}(\text{salen}^*)$  groups present in **2** and **4** attached to the lead ion show considerable overlap. Furthermore, only one nitrate ion in **2** and one acetate ion in **4** remain bonded to the lead center. Compound **3** is unique in that only one  $\text{Cu}(\text{salen}^*)$  group can bind to lead. Here, both acetate ligands remain attached, although one is chelating bidentate and the other is monodentate.

### Introduction

Many bimetallic or multimetallic oxide systems containing heavy main group metal and transition metals are being explored for the unique physical or chemical properties that these materials may possess. For example,  $\text{BiAlO}_3$  is an extremely efficient oxide ion conducting ceramic,<sup>1</sup> while  $\text{BaTiO}_3$  and  $\text{PbTi}_x\text{Zr}_{1-x}\text{O}_3$  are highly promising ferroelectric materials.<sup>2,3</sup> It has been shown by our group and others that discrete bimetallic coordination complexes can offer access to oxide materials at significantly reduced temperatures compared to what are required for traditional solid-state syntheses.<sup>4–10</sup> Additionally, the intimate mixing of the

different metal species in the complex generally prevents the formation of unwanted phases, allowing for the formation and isolation of the desired materials in much higher purity than what is generally accessible via traditional routes.<sup>11</sup>

One of the most significant challenges in developing the chemistry of heterobimetallic coordination complexes to act as potential precursors for the formation of oxide materials is the development of accessible synthetic approaches to these complexes that allow for control over the stoichiometry of the individual metal species with relationship to one another

\* Author to be contacted for correspondence. E-mail: whitmir@rice.edu. Phone: 713-348-5650. Fax: 713-348-5155.

- (1) Bloom, I.; Hash, M. C.; Zebrowski, J. P.; Myles, K. M.; Krumpelt, M. *Solid State Ionics* **1992**, *53–56*, 739–747.
- (2) Jones, A. C.; Chalker, P. R. *J. Physics D: Appl. Phys.* **2003**, *36*, R80–R95.
- (3) Schneller, T.; Waser, R. *Ferroelectrics* **2002**, *267*, 293–301.

- (4) Kessler, V. G. *Chem. Commun.* **2003**, *11*, 1213–1222.
- (5) Hubert-Pfaltzgraf, L. G. *Inorg. Chem. Commun.* **2003**, *6*, 102–120.
- (6) Hubert-Pfaltzgraf, L. G. *New J. Chem.* **1995**, *19*, 727–750.
- (7) Hubert-Pfaltzgraf, L. G. *Crit. Rev. Opt. Sci. Technol.* **1997**, *CR68*, 3–24.
- (8) Hubert-Pfaltzgraf, L. G.; Daniele, S.; Boulmaaz, S.; Papiernik, R. *Mater. Res. Soc. Symp. Proc.* **1994**, *346*, 21–27.
- (9) Thurston, J. H.; Whitmire, K. H. *Inorg. Chem.* **2002**, *41*, 4194–4205.
- (10) Thurston, J. H.; Whitmire, K. H. *Inorg. Chem.* **2003**, *42*, 2014–2023.
- (11) Veith, M. *J. Chem. Soc., Dalton Trans.* **2002**, *12*, 2405–2412.

in the final product.<sup>4</sup> In this regard, the formation of Lewis acid–base adducts is a particularly promising synthetic approach due to the generally high yields, relatively rapid reaction times, and absence of complicating side reactions. This approach has been successfully employed to produce heterobimetallic and heterotrimetallic coordination compounds.<sup>12–21</sup> As part of our ongoing studies into the development of the coordination chemistry of the heavy main group elements, we have investigated the reaction of a series of Pb(II) salts with M(salen)\* (M = Ni, Cu), and wish to report here the synthesis and characterization of the bimetallic coordination complexes Pb(Hsal)<sub>2</sub>·(Cu(salen\*))<sub>2</sub> (**1**), {Pb(NO<sub>3</sub>)·(Cu(salen\*))<sub>2</sub>}(NO<sub>3</sub>) (**2**), Pb(OAc)<sub>2</sub>·(Cu(salen\*)) (**3**), and {Pb(OAc)·(Ni(salen\*))<sub>2</sub>}(OAc) (Hsal = O<sub>2</sub>CC<sub>6</sub>H<sub>4</sub>-2-OH, salen\* = bis(3-methoxy)salicylideneimine). The new compounds have been characterized spectroscopically and by single-crystal X-ray diffraction experiments. Differences in the ligands attached to lead in the starting Pb<sup>2+</sup> salts as well as the nature of the metal in the M(salen\*) complexes influence the final stoichiometry and geometry of the products. The source of these differences will be discussed.

## Experimental Section

Solvents were purified over an appropriate reagent under argon and were distilled immediately prior to use.<sup>22</sup> The ligand bis(3-methoxy)salicylideneimine (H<sub>2</sub>salen\*) and the transition metal complexes copper(II)(salen\*) and nickel(II)(salen\*) were prepared as previously reported.<sup>23</sup> The starting materials lead(II) oxide, lead(II) acetate, lead(II) nitrate, copper(II) acetate, and nickel(II) acetate were purchased (Aldrich Chemical Co. or Strem Chemical Co.) and were used as received. Galbraith Laboratories performed all elemental analyses. NMR spectra were collected on a Bruker 400 Avance instrument and are referenced to tetramethylsilane (TMS) as an internal standard. Infrared spectra of the complexes were collected on a Thermo-Nicolet 630 FT-IR using ATR methodology. UV–vis data were collected on a GBC Spectral 918 instrument as dichloromethane solutions. Mass spectra were collected using matrix

assisted laser desorptive ionization–time-of-flight (MALDI-TOF) techniques on a Bruker Biflex III instrument, with a matrix of dithranol.

**Syntheses. Preparation of Lead(II) Salicylate.** A mixture of yellow lead(II) oxide (10.0 g, 45 mmol) and salicylic acid (13.8 g, 100 mmol) was placed in 200 mL of toluene. The suspension was heated to reflux for 24 h. During this time, the color of the suspension changed from yellow to white. The water that forms in the reaction was removed by azeotropic distillation using a Dean–Stark apparatus. After the reaction period, the solid was collected by filtration, washed repeatedly with diethyl ether (5 × 50 mL), and dried well under vacuum to give [Pb(Hsal)<sub>2</sub>]<sub>n</sub> as a white free flowing solid. Yield: 20 g (93%). FT-IR: 1620, 1587, 1543, 1518, 1481, 1457, 1398, 1387, 1359, 1301, 1249, 1224, 1153, 1145, 1030, 984, 952, 872, 819, 761, 754, 703. Elemental analysis: % obsd (% calcd for PbC<sub>14</sub>H<sub>10</sub>O<sub>6</sub>) C, 34.90 (35.01); H, 2.17 (2.09).

**Pb(Hsal)<sub>2</sub>·[Cu(salen\*)]<sub>2</sub> (**1**).** Compound **1** was synthesized by the addition of Cu(salen\*) (0.8 g, 2.0 mmol) to a suspension of [Pb(Hsal)<sub>2</sub>]<sub>n</sub> (0.47 g, 0.98 mmol), in dichloromethane (20 mL). The resulting burgundy solution was stirred until complete dissolution of the lead salt occurred, and then, the reaction mixture was allowed to stand undisturbed at room temperature for 24 h. The large burgundy crystals that deposited in the flask were collected by filtration, washed with dichloromethane and diethyl ether, and dried briefly under reduced pressure. Compound **1** yield: 0.92 g (0.73 mmol, 74%). Elemental analysis % obsd (% calcd for C<sub>46</sub>H<sub>46</sub>·Cu<sub>2</sub>N<sub>4</sub>O<sub>14</sub>Pb): C 45.12 (45.54), H 3.76 (3.82), N 4.45 (4.62). IR: 1635, 1622, 1602, 1590, 1562, 1484, 1471, 1456, 1447, 1400, 1381, 1353, 1320, 1303, 1290, 1246, 1223, 1170, 1140, 1082, 1028, 982, 961, 897, 863, 816, 806, 776, 756, 750, 734. This complex was essentially insoluble in organic solvents, precluding the measurement of solution spectroscopic data.

**{Pb(NO<sub>3</sub>)·(Cu(salen\*))<sub>2</sub>}(NO<sub>3</sub>) (**2**).** Compound **2** was synthesized in a manner analogous to **1** with the substitution of Pb(NO<sub>3</sub>)<sub>2</sub> for [Pb(Hsal)<sub>2</sub>]<sub>n</sub>. Large burgundy crystals of **2** were grown by slow evaporation of a dichloromethane solution of the compound. The solid was collected by filtration, washed with dichloromethane and diethyl ether, and dried briefly under reduced pressure. Compound **2** yield: 1.01 g (0.90 mmol, 92%). Elemental analysis: % obsd (% calcd for PbCu<sub>2</sub>C<sub>36</sub>H<sub>32</sub>N<sub>6</sub>O<sub>14</sub>·2H<sub>2</sub>O): C 37.22 (37.24); H 3.64 (3.13); N 7.21 (7.24). IR: 1618, 1601, 1554, 1480, 1467, 1446, 1395, 1368, 1309, 1280, 1242, 1221, 1163, 1140, 1078, 972, 869, 819, 771, 757, 737, 705, 667. MALDI-TOF MS: 985 (10%, 2 – NO<sub>3</sub> + Cu(salen\*)), 821 (100%, 2 – NO<sub>3</sub> + dithranol), 658 (90%, 2 – Cu(salen\*)), 390 (70%, Cu(salen\*)). ε<sub>0</sub> = 11 382 L·mol<sup>-1</sup>·cm<sup>-1</sup> at 362 nm in CH<sub>2</sub>Cl<sub>2</sub>.

**Pb(OAc)<sub>2</sub>·(Cu(salen\*)) (**3**).** Compound **3** was synthesized in a manner analogous to **1** with the substitution of Pb(OAc)<sub>2</sub> for [Pb(Hsal)<sub>2</sub>]<sub>n</sub>. Burgundy crystals of **3** were grown by slow evaporation of a dichloromethane solution of the compound in air. The solid was collected by filtration, washed with dichloromethane and diethyl ether, and dried briefly under reduced pressure. Compound **3** yield: 0.85 g (0.85 mmol, 83% based on Pb). Elemental analysis: % obsd (% calcd for PbCuC<sub>22</sub>H<sub>22</sub>O<sub>8</sub>N<sub>2</sub>·2H<sub>2</sub>O): C 35.18 (35.27), H 3.56 (3.23), N 3.70 (3.74). FT-IR (ATR): 1637, 1602, 1569, 1541, 1508, 1471, 1493, 1395, 1338, 1293, 1243, 1223, 1167, 1083, 1051, 1011, 984, 968, 923, 851, 781, 736. MALDI-TOF MS: 821 (100%, **3** – 2OAc + dithranol), 655 (50%, **3** – OAc), 596 (35%, **3** – 2OAc), 390 (20%, Cu(salen\*)). ε<sub>0</sub> = 17 567 L·mol<sup>-1</sup>·cm<sup>-1</sup> at 376 nm in CH<sub>2</sub>Cl<sub>2</sub>.

**{Pb(OAc)·(Ni(salen\*))<sub>2</sub>}(OAc) (**4**).** Compound **4** was synthesized in a manner analogous to **3** with the substitution of Ni(salen\*) for Cu(salen\*). Orange-red crystals of **4** were grown by slow

- (12) Ryazanov, M. V.; Troyanov, S. I.; Malkerova, I. P.; Alikhanyan, A. S.; Kuz'mina, N. P. *Zh. Neorg. Khim.* **2001**, *46*, 256–265.
- (13) Ryazanov, M.; Nikiforov, V.; Lloret, F.; Julve, M.; Kuzmina, N.; Gleizes, A. *Inorg. Chem.* **2002**, *41*, 1816–1823.
- (14) Kuz'mina, N. P.; Rogachev, A. Y.; Spiridonov, F. M.; Dedlovskaya, E. M.; Ketsko, V. A.; Gleizes, A.; Battiston, J. *Zh. Neorg. Khim.* **2000**, *45*, 1468–1475.
- (15) Gleizes, A. N.; Senocq, F.; Julve, M.; Sanz, J. L.; Kuzmina, N.; Troyanov, S.; Malkerova, I.; Alikhanyan, A.; Ryazanov, M.; Rogachev, A.; Dedlovskaya, E. *J. Phys. IV* **1999**, *9*, 943–951.
- (16) Gleizes, A.; Julve, M.; Kuzmina, N.; Alikhanyan, A.; Lloret, F.; Malkerova, I.; Sanz, J. L.; Senocq, F. *Eur. J. Inorg. Chem.* **1998**, 1169–1174.
- (17) Siddiqi, K. S.; Aqra, F. M. A. M.; Shah, S. A.; Zaidi, S. A. A.; Khan, N. H.; Kureshy, R. I. *Synth. React. Inorg. Met.-Org. Chem.* **1993**, *23*, 1645–1654.
- (18) Kondoh, N.; Shimizu, Y.; Kurihara, M.; Sakiyama, H.; Sakamoto, M.; Nishida, Y.; Sadaoka, Y.; Ohba, M.; Okawa, H. *Bull. Chem. Soc. Jpn.* **2003**, *76*, 1007–1008.
- (19) Sakamoto, M.; Manseki, K.; Okawa, H. *Coord. Chem. Rev.* **2001**, *219–221*, 379–414.
- (20) Kuzmina, N.; Ryazanov, M.; Malkerova, I.; Alikhanyan, A.; Gleizes, A. N. *Eur. J. Inorg. Chem.* **2001**, 701–706.
- (21) Sasaki, M.; Manseki, K.; Horiuchi, H.; Kumagai, M.; Sakamoto, M.; Sakiyama, H.; Nishida, Y.; Sakai, M.; Sadaoka, Y.; Ohba, M.; Okawa, H. *Dalton* **2000**, 259–263.
- (22) Armarego, W. L. F.; Perry, D. D. *Purification of Laboratory Chemicals*, 4th ed.; Butterworth-Heinemann: Boston, 1996.
- (23) Thurston, J. H.; Whitmire, K. H. *Chem. Mater.*, in press.

evaporation of a dichloromethane solution of the compound in air. The solid was collected by filtration, washed with dichloromethane and diethyl ether, and dried briefly under reduced pressure. Yield: 0.97 g (0.97 mmol, 76%).  $^1\text{H}$  NMR ( $\text{CDCl}_3$ , 400 MHz, 25 °C): 1.87 (s,  $\text{O}_2\text{CCH}_3$ , 6H), 2.00 (br, s,  $\text{H}_2\text{O}$ , 15H), 3.49 (s,  $-\text{CH}_2$ , 8H), 3.77 (s,  $-\text{OCH}_3$ , 12H), 6.48 (t, ArH, 4H,  $J = 7.85$  Hz), 6.66 (d, ArH, 4H,  $J = 7.41$  Hz), 6.71 (d, ArH, 4H,  $J = 7.88$  Hz).  $^{13}\text{C}\{^1\text{H}\}$  NMR ( $\text{CDCl}_3$ , 100 MHz, 25 °C): 55.56, 58.13, 113.19, 115.07, 120.29, 123.93, 151.76, 154.20, 159.85, 162.49, 179.87. Elemental analysis: % obsd (% calcd for  $\text{PbNi}_2\text{C}_{40}\text{H}_{38}\text{O}_{12}\text{N}_4 \cdot 7.5\text{H}_2\text{O}$ ) C, 38.80 (39.17); H, 4.57 (4.36); N, 4.64 (4.57). FT-IR (ATR): 1637, 1602, 1569, 1541, 1508, 1471, 1493, 1395, 1338, 1293, 1243, 1223, 1167, 1083, 1051, 1011, 984, 968, 923, 851, 781, 736. MALDI-TOF MS: 1040 (10%, **4** - OAc), 816 (100%, **4** - 2OAc + dithranol), 650 (35%, **4** - OAc - Ni(salen\*)), 591 (25%, PbNi(salen\*)), 385 (Ni(salen\*)).  $\epsilon_0 = 8641 \text{ L}\cdot\text{mol}^{-1}\cdot\text{cm}^{-1}$  at 353 nm in  $\text{CH}_2\text{Cl}_2$ .

**Solid-State Structures.** Compounds **1–4** were studied on a Bruker Smart 1000 diffractometer equipped with a CCD area detector. The data were corrected for Lorentz and polarization effects. An absorption correction was applied using the program SADABS.<sup>24</sup> No appreciable decay of the crystals was detected during data collection. Heavy atoms in the compounds were located using Patterson methods with the SHELXTL software package.<sup>25</sup> All other atoms were located by successive Fourier difference maps and were refined using the full-matrix least-squares technique on  $F^2$ . All non-hydrogen atoms were refined anisotropically. Hydrogen atoms in all of the complexes were placed in calculated positions and allowed to ride on the adjacent atom. Hydrogen atoms associated with phenolic oxygen atoms were placed in calculated positions and refined geometrically using a riding model. The hydrogen atom was oriented so that the most likely hydrogen bond, in this case to a carboxylate oxygen of the same molecule, was realized. The presence of intermolecular hydrogen bonding in the complexes was explored using the program PLATON.<sup>26</sup>

In the course of structure solution and refinement of complexes **2** and **4**, only one of the two anions (those coordinated to the lead center) could be located from the Fourier map of the residual electron density. Analysis of the packing behavior of these two compounds reveals that, in the solid state, they form weak pseudo-one-dimensional polymeric assemblies. In the case of **2**, the intermolecular interactions are  $\pi$  stacking forces between salen\* ligands, while in **4**, there are apparent weak Ni $\cdots$ Ni interactions. The displaced anions, in addition to any lattice water that might be present (presence of small amounts of lattice water were confirmed by NMR and were included in calculating the elemental analyses), are presumably located in the interstitial spaces of the crystal lattice, as suggested by the high residual electron density that is found in these areas. However, the displaced anions are subject to disorder and could not be located. Consequently, the electron density associated with this fragment was artificially subtracted from the data set using the program SQUEEZE.<sup>26</sup> The composition of the compounds was confirmed through both elemental analysis and spectroscopic techniques. The complete elucidation of these two compounds is discussed in more depth in the Results section.

## Results

Divalent lead salts react smoothly with transition metal salen\* complexes to produce stable heterobimetallic coor-

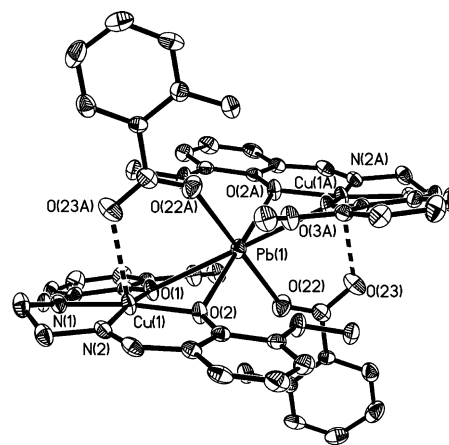


**Figure 1.** ORTEP representation of the solid-state structure of **1**. Thermal ellipsoids are drawn at the 30% probability level. Hydrogen atoms have been omitted for clarity. Broken lines represent dative interactions between salen\* ligands and copper(II) centers.

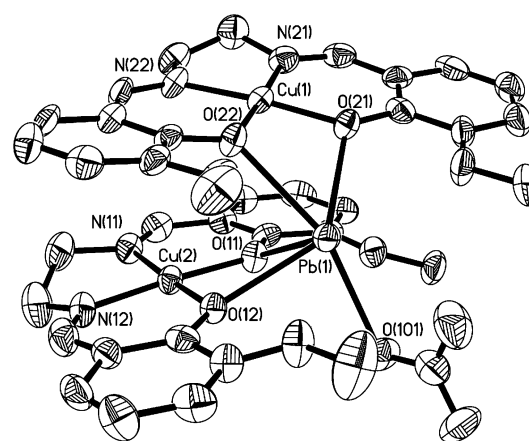


**Figure 2.** ORTEP representation of the cation of **2**. Thermal ellipsoids are drawn at the 30% probability level, and hydrogen atoms have been omitted for clarity.

dination compounds. The structure and composition of these compounds, as determined spectroscopically and by single-crystal X-ray diffraction experiments, vary dramatically both with changes in the lead salt and with changes in the transition metal salen\* compounds. The structures of the compounds, as determined by single-crystal X-ray diffraction experiments, are provided in Figures 1–6, while pertinent details relating to the data collection and refinement are provided in Tables 1–5.

The lead center in all of the compounds developed in this study interacts with the transition metal salen\* complexes through the phenoxy groups of the salen\* ligand. The Pb– $\text{O}_{\text{salen}}$  bond lengths in compounds **1–4** range from 2.479(3) to 2.971(5) Å and are similar to the bond distances observed for other main group metal–transition metal salen\* complexes that have been produced by our group and by others;<sup>14,16,23</sup> however, the interaction of the lead with the two oxygen atoms is asymmetric, and in the case of **3**, the second interaction is so much weaker than the first ( $d_{\text{Pb-O}} = 2.479(3)$  and 2.971(5) Å) (Figure 3) that the Cu(salen\*) might be more appropriately considered as essentially a monodentate ligand. In compounds **1–4**, the angle between the  $\text{O}_{\text{salen}^*}\text{–Pb–O}_{\text{salen}^*}$  plane and the plane defined by the

(24) SADABS; University of Göttingen: Göttingen, Germany, 1997.

(25) SHELXTL; University of Göttingen: Göttingen, Germany, 2001.

(26) Spek, A. *Platon, A Multipurpose Crystallographic Tool*; Utrecht: The Netherlands, 2001.

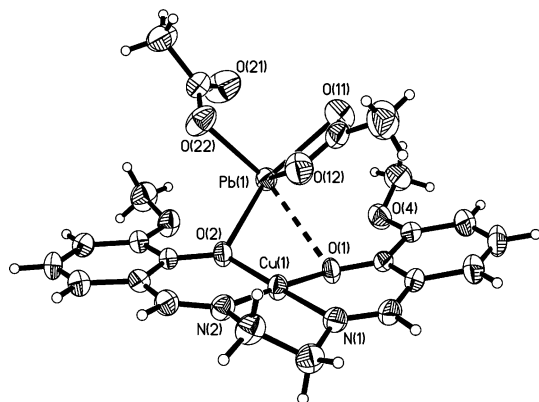


**Figure 3.** ORTEP representation of complex **3**. Thermal ellipsoids are drawn at the 50% probability level. A broken line represents weak interactions between Pb(1) and O(1). Lattice solvent has been omitted for clarity.

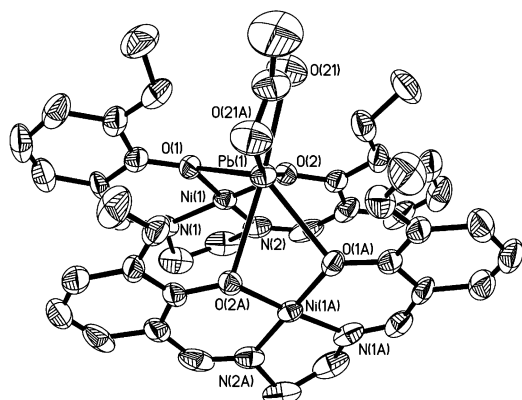


**Figure 4.** ORTEP representation of the cation of complex **4**. Thermal ellipsoids have been drawn at the 30% probability level, and hydrogen atoms have been omitted for clarity.

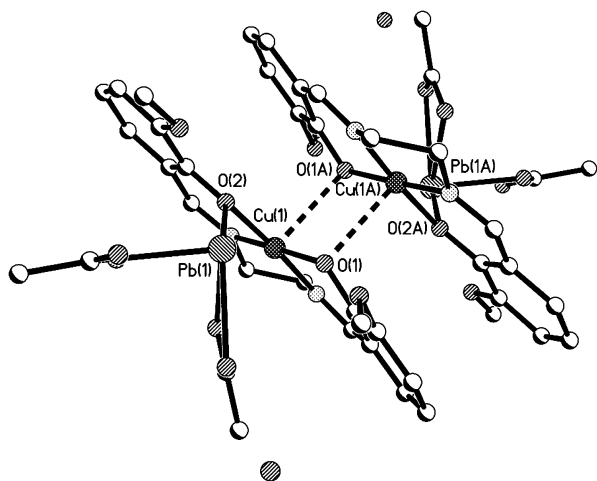


**Figure 5.** Ball-and-stick representation of the packing orientation of **3**. Hydrogen atoms have been omitted for clarity. Broken lines represent short contacts between copper atoms and phenolic oxygen atoms.

salen\* ligand ranges from ca. 143.6° to 154.8°, indicating that the lead center sits well out of the plane of the salen\* ligand. This orientation of the lead presumably maximizes the interaction of the main group metal with the phenolic oxygen lone pair electrons and is similar to what has been observed in other complexes.<sup>23</sup> The stability of the Pb–M(salen\*) interactions is strong enough that the parent ion,

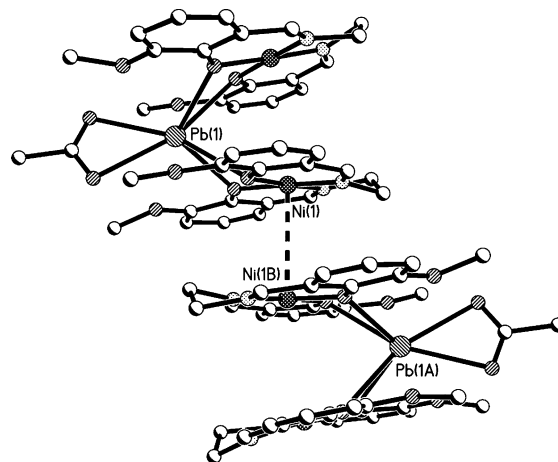


**Figure 6.** Ball-and-stick representation of the packing orientation of **4**. Short Ni–Ni contacts in the crystal lattice are illustrated by broken lines. Hydrogen atoms have been omitted for clarity.

**Table 1.** Crystallographic Data for New Compounds

	1	2	3	4
formula	C <sub>50</sub> H <sub>46</sub> Cu <sub>2</sub> -N <sub>4</sub> O <sub>14</sub> Pb	C <sub>36</sub> H <sub>36</sub> Cu <sub>2</sub> -N <sub>6</sub> O <sub>10</sub> Pb	C <sub>22</sub> H <sub>26</sub> Cu-N <sub>2</sub> O <sub>9</sub> Pb	C <sub>38</sub> H <sub>39</sub> N <sub>4</sub> -Ni <sub>2</sub> O <sub>10</sub> Pb
fw	1261.18	1126.98	733.16	1064.86
space group	<i>P</i> $\bar{1}$	<i>Pbca</i>	<i>P</i> $\bar{1}$	<i>C2/c</i>
Z	1	8	2	4
cryst syst	triclinic	orthorhombic	triclinic	monoclinic
<i>a</i> (Å)	10.480(2)	22.868(5)	9.990(2)	18.688(4)
<i>b</i> (Å)	10.515(2)	15.543(3)	10.759(2)	26.355(5)
<i>c</i> (Å)	11.988(2)	23.434(5)	12.756(3)	13.377(3)
$\alpha$ (deg)	71.50(3)		110.96(3)	
$\beta$ (deg)	64.50(3)		103.97(3)	133.01(3)
$\gamma$ (deg)	79.52(3)		97.73(3)	
<i>V</i> , Å <sup>3</sup>	1129.1(4)	8329(3)	1188.0(4)	4818.0(17)
<i>D</i> (calcd), g/mm <sup>3</sup>	1.855	1.698	2.044	1.468
temp (°C)	28	28	28	28
$\lambda$ , Mo K $\alpha$ (Å)	0.71073	0.71073	0.71073	0.71073
$\mu$ (cm <sup>-1</sup> )	47.29	51.08	80.27	43.14
<i>R</i> <sup>1</sup> <sup>a</sup>	0.0352	0.0582	0.0196	0.0533
<i>wR</i> <sup>2</sup> <sup>b</sup>	0.0728	0.2004	0.0509	0.1626

<sup>a</sup> Conventional *R* on  $F_{hkl}$ :  $\sum |F_o| - |F_c| / \sum |F_o|$ . <sup>b</sup> Weighted *R* on  $|F_{hkl}|^2$ :  $\{\sum [w(F_o^2 - F_c^2)^2] / \sum [w(F_o^2)^2]\}^{1/2}$ .

**Table 2.** Selected Bond Lengths [Å] and Angles [deg] for **1**<sup>a</sup>

Pb(1)–O(1)	2.690(4)	Cu(1)–O(2)	1.906(4)
Pb(1)–O(2)	2.579(4)	Cu(1)–N(1)	1.905(5)
Pb(1)–O(22)	2.545(5)	Cu(1)–N(2)	1.938(5)
Cu(1)–O(1)	1.910(4)		
O(1)#1–Pb(1)–O(1)	180.00(16)	O(22)#1–Pb(1)–O(2)#1	99.73(15)
O(2)–Pb(1)–O(1)#1	120.46(11)	O(22)–Pb(1)–O(2)	99.73(15)
O(2)#1–Pb(1)–O(1)	120.46(11)	O(22)#1–Pb(1)–O(2)	80.27(15)
O(2)–Pb(1)–O(1)	59.54(11)	O(1)–Cu(1)–N(2)	172.45(19)
O(2)#1–Pb(1)–O(2)	180.00(12)	O(2)–Cu(1)–O(1)	86.65(15)
O(2)#1–Pb(1)–O(1)#1	59.54(11)	O(2)–Cu(1)–N(2)	93.35(18)
O(22)–Pb(1)–O(1)	92.51(14)	N(1)–Cu(1)–O(2)	173.5(2)
O(22)#1–Pb(1)–O(1)	87.49(14)	N(1)–Cu(1)–O(1)	94.45(19)
O(22)–Pb(1)–O(1)#1	87.49(14)	N(1)–Cu(1)–N(2)	84.7(2)
O(22)#1–Pb(1)–O(1)#1	92.51(14)	Cu(1)–O(1)–Pb(1)	97.31(14)
O(22)–Pb(1)–O(22)#1	180.000(1)	Cu(1)–O(2)–Pb(1)	101.19(15)
O(22)–Pb(1)–O(2)#1	80.27(15)		

<sup>a</sup> Symmetry transformations used to generate equivalent atoms: #1  $-x + 1, -y + 1, -z + 1$ .

plus several daughter fragments of each of these compounds, is observed in the MALDI-TOF mass spectra.

As noted above, the geometry at the lead center varies dramatically both under the influence of the lead salt and under the influence of the transition metal salen\* compound.

**Table 3.** Selected Bond Lengths [Å] and Angles [deg] for **2**

Pb(1)–O(11)	2.481(8)	Cu(1)–N(21)	1.913(11)
Pb(1)–O(12)	2.604(7)	Cu(1)–N(22)	1.914(11)
Pb(1)–O(21)	2.637(8)	Cu(2)–O(11)	1.891(8)
Pb(1)–O(22)	2.648(8)	Cu(2)–N(12)	1.908(11)
Pb(1)–O(101)	2.651(11)	Cu(2)–O(12)	1.910(8)
Cu(1)–O(21)	1.889(8)	Cu(2)–N(11)	1.913(12)
Cu(1)–O(22)	1.911(8)		
O(11)–Pb(1)–O(12)	61.1(2)	O(22)–Cu(1)–N(22)	94.4(4)
O(11)–Pb(1)–O(21)	82.2(3)	N(21)–Cu(1)–N(22)	84.3(5)
O(12)–Pb(1)–O(21)	130.5(3)	O(11)–Cu(2)–N(12)	176.2(4)
O(11)–Pb(1)–O(22)	71.8(3)	O(11)–Cu(2)–O(12)	85.7(3)
O(12)–Pb(1)–O(22)	78.4(3)	N(12)–Cu(2)–O(12)	94.5(4)
O(21)–Pb(1)–O(22)	58.3(3)	O(11)–Cu(2)–N(11)	94.9(4)
O(11)–Pb(1)–O(101)	84.4(3)	N(12)–Cu(2)–N(11)	85.2(5)
O(12)–Pb(1)–O(101)	85.2(3)	O(12)–Cu(2)–N(11)	175.8(4)
O(21)–Pb(1)–O(101)	125.2(3)	Cu(2)–O(11)–Pb(1)	105.6(3)
O(22)–Pb(1)–O(101)	155.6(3)	Cu(2)–O(12)–Pb(1)	100.5(3)
O(11)–Cu(1)–O(22)	85.2(3)	Cu(1)–O(21)–Pb(1)	101.7(3)
O(21)–Cu(1)–N(21)	96.3(4)	Cu(1)–O(22)–Pb(1)	100.7(3)
O(22)–Cu(1)–N(21)	177.1(4)	N(100)–O(101)–Pb(1)	108.1(9)
O(21)–Cu(1)–N(22)	175.4(4)		

**Table 4.** Selected Bond Lengths [Å] and Angles [deg] for **3**

Pb(1)–O(2)	2.479(3)	Cu(1)–O(1)	1.928(3)
Pb(1)–O(11)	2.433(3)	Cu(1)–O(2)	1.923(3)
Pb(1)–O(12)	2.584(3)	Cu(1)–N(1)	1.929(3)
Pb(1)–O(21)	2.356(3)	Cu(1)–N(2)	1.940(3)
O(21)–Pb(1)–O(11)	77.48(12)	O(2)–Cu(1)–N(1)	175.87(13)
O(21)–Pb(1)–O(2)	86.87(11)	O(1)–Cu(1)–N(1)	92.84(13)
O(11)–Pb(1)–O(2)	74.23(10)	O(2)–Cu(1)–N(2)	93.18(13)
O(21)–Pb(1)–O(12)	88.27(12)	O(1)–Cu(1)–N(2)	176.92(12)
O(11)–Pb(1)–O(12)	51.62(12)	N(1)–Cu(1)–N(2)	84.08(14)
O(2)–Pb(1)–O(12)	125.32(11)	Cu(1)–O(2)–Pb(1)	106.69(11)
O(2)–Cu(1)–O(1)	89.90(11)		

**Table 5.** Selected Bond Lengths [Å] and Angles [deg] for **4**<sup>a</sup>

Pb(1)–O(1)	2.613(7)	Ni(1)–O(2)	1.841(7)
Pb(1)–O(2)	2.633(7)	Ni(1)–O(1)	1.844(8)
Pb(1)–O(21)	2.663(10)	Ni(1)–N(1)	1.854(11)
Ni(1)–N(2)	1.826(11)		
O(1)#1–Pb(1)–O(1)	113.9(3)	O(2)–Pb(1)–O(21)	112.8(3)
O(1)#1–Pb(1)–O(2)	76.7(2)	O(2)#1–Pb(1)–O(21)	160.6(3)
O(1)–Pb(1)–O(2)	55.6(2)	O(21)#1–Pb(1)–O(21)	47.8(5)
O(1)#1–Pb(1)–O(2)#1	55.6(2)	N(2)–Ni(1)–O(2)	95.7(5)
O(1)–Pb(1)–O(2)#1	76.7(2)	N(2)–Ni(1)–O(1)	178.1(4)
O(2)–Pb(1)–O(2)#1	86.5(3)	O(2)–Ni(1)–O(1)	83.2(3)
O(1)#1–Pb(1)–O(21)#1	113.4(3)	N(2)–Ni(1)–N(1)	86.6(6)
O(1)–Pb(1)–O(21)#1	126.9(3)	O(2)–Ni(1)–N(1)	176.8(4)
O(2)–Pb(1)–O(21)#1	160.6(3)	O(1)–Ni(1)–N(1)	94.5(5)
O(2)#1–Pb(1)–O(21)#1	112.8(3)	Ni(1)–O(1)–Pb(1)	103.7(3)
O(1)#1–Pb(1)–O(21)	126.9(3)	Ni(1)–O(2)–Pb(1)	103.0(3)
O(1)–Pb(1)–O(21)	113.4(3)		

<sup>a</sup> Symmetry transformations used to generate equivalent atoms: #1  $-x, y, -z + 1/2$ .

The influence of the anion on the coordination environment of the lead center in the heterobimetallic complexes is succinctly illustrated in the solid-state structures of compounds **1–3**. Interaction of lead(II) salicylate with Cu(salen<sup>\*</sup>) results in the formation of the neutral 2:1 adduct **1**. In this case, the lead is six-coordinate and adopts a distorted octahedral coordination environment in which four of these sites are occupied by the two Cu(salen<sup>\*</sup>) ligands and two by the monodentate salicylate ligands that are oriented *trans* to one another. These salicylate ligands also bridge to the Cu<sup>2+</sup> ions.

Compounds **2** and **4** resemble **1** in that they are also 2:1 adducts; however, in these compounds the interaction of the M(salen<sup>\*</sup>) complex (M = Cu, Ni) with the lead salt results in displacement of one of the anions. Additionally, there is a significant difference in the orientations of the two salen<sup>\*</sup> ligands in **1**, **2**, and **4**. In the solid-state structure of **1**, the salen<sup>\*</sup> ligands are directly opposed to one another as imposed by crystallographic inversion symmetry, and consequently, the Cu<sup>⋯</sup>Pb<sup>⋯</sup>Cu angle is exactly 180.0°. In contrast to this orientation, the Cu<sup>⋯</sup>Pb<sup>⋯</sup>Cu angles in **2** and **4** are ca. 71.8° and 63.4°, respectively, reflecting that the M(salen<sup>\*</sup>) ligands overlap to a significant extent that does not occur for **1**.

A subtle difference between compounds **2** and **4** lies in the nature of the interaction of the coordinated anion with the lead center. In the case of **2**, the nitrate ion adopts a monodentate interaction with the lead, whereas in the case of **4**, the acetate adopts a bidentate chelating coordination mode. As a result of the different coordination modes of the anions in these complexes, the lead center in compound **2** can be most effectively described as adopting a distorted square pyramidal geometry whereas the lead center in compound **4** is a distorted trigonal pyramid.

It is important to note that the solid-state structures of compounds **2** and **4** indicate that the association of the M(salen<sup>\*</sup>) complex with the lead center results in the displacement of one of the anions from the lead center, and consequent formation of an ionic complex. As noted above, we were not able to locate the anions directly from the residual electron density due to disordering of the remaining counterion. Both structures show large vacant channels, and presumably, the counterions are dispersed throughout these spaces in a highly disordered fashion. Confirmation of the identity of the displaced anions has been achieved by elemental analysis, in which the observed composition shows excellent agreement with the values predicted from the proposed formulas. Additionally, spectroscopic interrogation of **4** by multinuclear NMR studies reveals a 1:1 ratio of acetate to salen<sup>\*</sup>, consistent with our formulation for this compound. Similar analysis was not possible for **2** owing to the presence of the paramagnetic Cu<sup>2+</sup> ion.

Complex **3** is unique in this study as it is the only 1:1 adduct that was produced under the conditions explored. As noted above, the interaction of the salen<sup>\*</sup> compound with the lead center is highly asymmetric resulting in the geometry at the lead center being intermediate to that of a distorted tetrahedron and a distorted trigonal bipyramid. In addition to the transition metal compound, the coordination environment of the lead is completed by interactions with the two acetate ions, one of which is monodentate, while the other is bidentate and chelating. The general structural and geometric parameters of the four complexes developed in this study, including Pb–O bond lengths and angles, all agree well with what was anticipated from the reports of other similar complexes.<sup>14,16,17,23</sup>

An additional consideration in this regard is that the identity and consequent electronic structure of the transition metal appears to assert some influence on the overall packing structure of the complexes. The Cu(salen<sup>\*</sup>) complexes in

compounds **1** and **3** contain five-coordinate copper atoms. In the case of compound **1**, the coordination sphere of the copper is completed intramolecularly by the bridging salicylate ligands. Complex **3**, on the other hand, is observed to pack so that the apical coordination site of the five-coordinate copper center is occupied by a phenolic oxygen in an adjacent salen\* ligand (Figure 5). Some additional stabilization of this packing mode may arise from  $\pi$  stacking interactions between adjacent salen\* ligands ( $d_{\text{centroid-centroid}} = 3.827(4)$  Å). Unlike compounds **1** and **3**, the copper centers in complex **2** adopt strictly four-coordinate, square planar geometries. The reasons for the different coordination requirements of the copper in these compounds are not clear at this point.

In contrast to the packing behavior of the Cu(salen\*) compounds, complex **4** is observed to adopt an orientation in the crystal lattice that affords short intermolecular Ni–Ni contacts ( $d_{\text{Ni-Ni}} = 3.497(3)$  Å) (Figure 6). It is important to note that the packing behavior of all four complexes, particularly with regard to the formation of close intermolecular ring contacts in the copper systems or metal–metal contacts in the nickel systems, is in accord with similar compounds that have been prepared by our group and others.<sup>14,16,23</sup>

## Discussion

The composition and geometry of the complexes produced in this study can be most directly viewed as arising from a competition between the anion and the salen\* complexes for coordination with the lead center. The influence of this competition can be seen in the solid-state structures of complexes **1**–**3**. The anions employed in this study range from the nonbasic NO<sub>3</sub><sup>−</sup> ion to the somewhat more strongly basic salicylate ligand ( $pK_{\text{a1}}$ , salicylic acid = 2.75) to the acetate ion ( $pK_{\text{a}}$ , acetic acid = 4.74). The acetate ion, which is the most strongly coordinating, is able to compete efficiently with the salen\* ligands for interaction with the lead center, resulting in the formation of the 1:1 adduct **3**. It is important to note that complex **3** is the only heterobimetallic compound that is produced in this reaction, even if an excess of Cu(salen\*) is employed. In contrast, the weakly coordinating nitrate ligand is readily displaced from the lead coordination sphere in the case of complex **2**, and the 2:1 adduct **2** is obtained as the sole product. As expected from the relative  $pK_{\text{a}}$  of the salicylate ligand, complex **1** is structurally intermediate between compounds **2** and **3**. The salicylate ligands are basic enough that they are not displaced completely, similar to **3**, but the coordination mode of the carboxylate anions is now monodentate, as opposed to the bidentate chelating interaction that is more commonly encountered in main group carboxylate coordination chemistry. As was observed for complex **3**, the 2:1 adduct **1** is

the only heterobimetallic complex produced from the reaction, even if only 1 equiv of Cu(salen\*) is employed in the synthesis.

In addition to the effects of the anions, the electronic environment of the salen\* ligand also appears to have a profound impact on the composition and resulting structure of these coordination compounds. This is most clearly illustrated in the case of complexes **3** and **4**, in which the only chemical difference between the starting reagents is the electronic environment of the two transition metals. As noted above, complex **3** consists of a neutral 1:1 adduct in which both acetate anions are bound to the lead center. In contrast, compound **4** consists of an ionic 2:1 adduct in which one of the acetate anions has been displaced from the lead coordination sphere, while the remaining anion adopts a bidentate chelating coordination mode. The compositional differences between these two molecules likely arise from the differences in the relative acidities of the two different transition metal centers (cf.,  $pK_{\text{a}}$  Cu(H<sub>2</sub>O)<sub>6</sub><sup>2+</sup>(aq) = 7.49,  $pK_{\text{a}}$  Ni(H<sub>2</sub>O)<sub>6</sub><sup>2+</sup>(aq) = 9.03).<sup>27</sup> The less acidic Ni<sup>2+</sup> ion would be expected to produce greater electron density at the phenolic oxygen atoms, allowing it to bind more effectively to the lead center than the Cu(salen\*) complex, resulting in displacement of an acetate ion. The shorter Pb–O<sub>salen</sub> bond distances that are observed in **3** as opposed to **4** (**3**:  $d_{\text{Pb-O}} = 2.479(3)$  Å, **4**:  $d_{\text{Pb-O}} = 2.613(7)$  and  $2.633(7)$  Å) are believed to stem from steric interactions relating to the orientation of the relatively bulky salen\* complex in the lead coordination sphere when two such ligands are present. Additionally, it is possible that the presence of two transition metal salen\* complexes attenuates that Lewis acidity of the lead center, resulting in weaker binding of the transition metal complex.

## Conclusions

The results of this study indicate that the formation of heterobimetallic coordination complexes via Lewis acid–base interactions can be accurately viewed as arising from a direct competition between an M(salen\*) complex and acetate, salicylate, or nitrate for binding to a lead center. Clearly, precisely tuning the composition of heterobimetallic coordination complexes through careful selection of both the metal species and the respective ligands is possible. Additionally, the apparent generality of this chemistry suggests that it may be possible to apply these techniques to a wide variety of metal species. Similar results have been obtained for coordination of M(acac)<sub>3</sub> (acac = 2,4-pentanedionate<sup>−1</sup>) complexes bound to bismuth salicylate.<sup>28</sup> In this manner, it may be possible to move beyond “fortuitous self-assembly” in the design of molecular precursors for the formation of advanced materials.

**Acknowledgment.** We would like to thank the Robert A. Welch Foundation and the National Science Foundation CHE-9983352 for support of this work.

**Supporting Information Available:** Crystallographic data in CIF format. This material is available free of charge via the Internet at <http://pubs.acs.org>.

IC035427W

(27) *Lange's Handbook of Chemistry*, 15th ed.; McGraw-Hill: New York, 1999.

(28) Thurston, J. H.; Trahan, D. W.; Ould Ely, T.; Whitmire, K. H. *Inorg. Chem.*, submitted for publication.